

In vitro and in vivo antitumor effects of the VO-chrysin complex on a new three-dimensional osteosarcoma spheroids model and a xenograft tumor in mice

Ignacio E. León^{1,2} · Juan F. Cadavid-Vargas^{1,2} · Agustina Resasco³ · Fabricio Maschi³ · Miguel A. Ayala³ · Cecilia Carbone³ · Susana B. Etcheverry^{1,2}

Received: 2 June 2016 / Accepted: 16 September 2016 / Published online: 1 October 2016
© SBIC 2016

Abstract Osteosarcoma (OS) is the most common primary tumor of bone, occurring predominantly in the second decade of life. High-dose cytotoxic chemotherapy and surgical resection have improved prognosis, with long-term survival for patients with localized disease. Vanadium is an ultra-trace element that after being absorbed accumulates in bone. Besides, vanadium compounds have been studied during recent years to be considered as representative of a new class of non-platinum antitumor agents. Moreover, flavonoids are a wide family of polyphenolic compounds that display many interesting biological effects. Since coordination of ligands to metals can improve the pharmacological properties, we report

herein, for the first time, the in vitro and in vivo effects of an oxidovanadium(IV) complex with the flavonoid chrysin on the new 3D human osteosarcoma and xenograft osteosarcoma mice models. The pharmacological results show that VOchrys inhibited the cell viability affecting the shape and volume of the spheroids and VOchrys suppressed MG-63 tumor growth in the nude mice without inducing toxicity and side effects. As a whole, the results presented herein demonstrate that the antitumor action of the complex was very promissory on human osteosarcoma models, whereby suggesting that VOchrys is a potentially good candidate for future use in alternative antitumor treatments.

Electronic supplementary material The online version of this article (doi:[10.1007/s00775-016-1397-0](https://doi.org/10.1007/s00775-016-1397-0)) contains supplementary material, which is available to authorized users.

✉ Ignacio E. León
ileon@biol.unlp.edu.ar

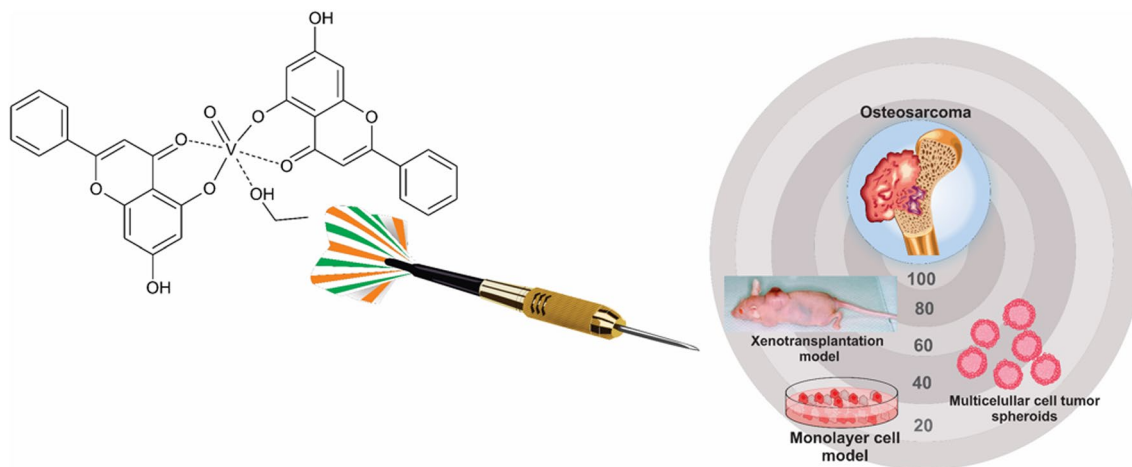
✉ Susana B. Etcheverry
etcheverry@biol.unlp.edu.ar

¹ Cátedra de Bioquímica Patológica, Facultad Ciencias Exactas, Universidad Nacional de La Plata, 47 y 115, 1900 La Plata, Argentina

² Centro de Química Inorgánica (CEQUINOR-CONICET), Facultad de Ciencias Exactas, Universidad Nacional de La Plata, 47 y 115, 1900 La Plata, Argentina

³ Cátedra de animales de laboratorio, Facultad de Ciencias Veterinarias, Universidad Nacional de La Plata, 60 y 118, 1900 La Plata, Argentina

Graphical Abstract



Keywords Osteosarcoma · Vanadium · Xenograft mice · Spheroids · Flavonoids

Introduction

Vanadium is an ultra-trace element present in higher plants and animals [1].

The biological effects of vanadium convert its compounds in potential therapeutic agents to be used in the treatment of a number of diseases, such as diabetes [2–4], osteoporosis [5], and cancer [6–9]. In vertebrates, after absorption and tissue distribution, great amounts of vanadium are detected in liver and especially in bone [1].

Osteosarcoma (OS) is a primary bone malignant tumor, and it is the most common bone tumor in children and young adults [10]. To improve the welfare and survival of the patients, a more comprehensive understanding of the mechanisms underlying the clinical expression of OS is of great importance to identify novel chemotherapeutic drugs for a more effective treatment.

The use of monolayer cultures applied to test potential anticancer drugs is one of the most useful employed techniques. However, this model has a lack of high similarity, since the cells are organized in two dimensions [11]. In the bidimensional cultures, the cells are more likely to be affected by the substance under evaluation than in more representative models for tumors [12]. Due to the limitations to test substances in monolayer culture, the need of a reliable model that mimics the tumor tissue organization is of great interest. This approach allows the scientists to handle a high-throughput, pushing for the development of 3D models that show the basic characteristics of tumors [13]. The multicellular spheroids (MCS), as a 3D model

of tumor, simulate the avascular or micrometastatic state of an *in vivo* tumor [14]. This kind of 3D tumor model is widespread to study the transport and cell uptake of antitumor based drugs [15, 16]. Currently, Hambleys group uses several spectroscopic imaging and mapping techniques to characterize the spheroid solid tumors [17].

On the other hand, animal models of human cancers are very helpful to elucidate the multifaceted mechanisms relevant for tumor development. These mechanisms cannot properly be addressed in other systems, including monolayers and 3D tumor spheroids [18]. Moreover, animal models are essential tools for the design and development of new drugs for cancer diagnostic and treatment in preclinical research [19].

In the last few decades, vanadium compounds have been considered as a new class of metal-based antitumor agents, but the effects of these compounds in 3D *in vitro* and *in vivo* systems are scarcely reported and examined in the literature.

As part of a project related to the research of vanadium compounds with potential therapeutic applications, this study deals with the effects of an oxidovanadium(IV) complex with the flavonoid chrysin, $[\text{VO}(\text{chrysin})_2\text{EtOH}]_2$ on 3D multicellular spheroids and osteosarcoma cell xenograft in mice. For the first time, we have investigated and reported herein the action of VOchry on the viability of MG-63 osteosarcoma cells (multicellular spheroids and xenograft mice). This tumor cell line derived from a human source is a very good model to study the antitumor actions involved in the antiproliferative effects of new compounds. In particular, we focus our investigation on the development of models of MG-63 multicellular spheroids and xenograft mice to get further pharmacological evaluation of this promissory vanadium-flavonoid compound.

Materials and methods

Experiment

Synthesis of VOchrys

VOchrys was synthesized according to previously reported results [20]. Briefly, chrysin (0.5 mmol) was mixed with vanadyl acetylacetonate (0.25 mmol) in absolute ethanol and refluxed for ca. 1.30 h (final pH = 5). The hot green suspension was filtered; the solid was washed three times with absolute ethanol and air-dried. Anal. Calc. for $C_{64}H_{48}O_{20}V_2$: C, 62.0; H, 3.9; V, 8.2. Exp.: C, 62.2; H, 4.3; V, 8.2. Yield: 72 %.

The identification of the complex was done by FTIR following the main absorption bands of the complex [ν (V=O) 967 cm^{-1} , ν (C=O) 1630 cm^{-1} , Ring B, and δ_{ip} (CH) 1521 cm^{-1}].

Preparation of VOchrys solutions

Fresh stock solutions of the complex (20 mM) were prepared in DMSO and diluted according to the concentrations indicated in the legends of the figures.

Cell culture

The human osteosarcoma (MG-63) cell line was purchased from ATCC (CRL1427TM). Cells were grown in DMEM containing 10 % FBS, 100 U mL⁻¹ penicillin, and 100 $\mu\text{g mL}^{-1}$ streptomycin at 37 °C in a 5 % CO₂ atmosphere. Cells were seeded in a 25 cm² flask, and when 70–80 % of confluence was reached, cells were subcultured (1 mL TrypLETM per 25 cm² flask).

Multicellular spheroids formation

The development of multicellular spheroids was achieved by the hanging drop technique [21] with minor modifications. Briefly, a flask with growing cells was rinsed with sterile PBS, and then, 1 mL of TrypLETM was added to harvest the cells. The cell suspension was adjusted to a concentration of 60 cells/ μL ; this concentration was selected to get 400 μm diameter spheroids at the beginning of the treatment with the compound. After 48 h, the compacted spheroids were transferred to an agar coated 96-well plate, and then, 200 μL of DMEM plus 10 % FBS were added to each well. The plate was cultured under the standard conditions for eight days, replacing 50 % of the culture media every 48 h.

Vanadium treatment of multicellular spheroids

For pharmacologic experiments, multicellular spheroids were treated in 96-well plates with 1 % DMSO in DMEM plus 10 % FBS (basal conditions) and 100 μM of VOchrys in DMEM plus 10 % FBS (treatment condition) for 72 h. After that, the evaluation of damage in the cell viability of spheroids was achieved by the acid phosphatase assay and image analysis.

Acid phosphatase assay

To determine in a reliable and high-throughput way the viability [22] of the cells within the spheroids, we used this technique, since it is known that living cells express acid phosphatase. This enzyme catalyzes the hydrolysis of *p*-nitro-phenyl phosphate to *p*-nitrophenol, and the absorbance of this substance can be measured at 405 nm and used to quantify the surviving cells after the treatment [14]. The color development was measured spectrophotometrically at 405 nm with a microplate reader (model 7530, Cambridge Technology, USA).

Phase contrast microscopy and image analysis

Phase contrast microphotographs of each MCS were taken before and after the treatment using an Olympus IX51 inverted microscope with a digital camera of eight megapixels resolution attached to a personal computer. The image processing was performed under the software ImageJ. For comparative purposes and normalization of the data, we employed the factor shape corrected volume, calculated by the following equation:

$$V' = \text{Circularity} \times \text{volume} \quad (1)$$

where:

$$\text{Volume} = \frac{4}{3} \times \pi \times r^3 \quad (2)$$

$$\text{Circularity} = 4\pi \times \frac{\text{area}}{\text{perimeter}^2} \quad (3)$$

Ethics statement

The animal study was conducted in accordance with the Guide for the Care and Use of Laboratory Animals of the National Research Council, USA [23].

The Animal Lab Care Committee (IACUC) of Veterinary School, National University of La Plata has approved all animal protocols used in this research (E36-3-13). All surgeries

were performed under ketamine–xylazine (100 mg–20 mg/kg) anesthesia. All efforts were made to minimize animal suffering, to decrease the number of animals used, and to utilize possible alternatives to in vivo techniques.

Tumor implantation, treatment, and evaluation

Xenograft tumors were established in 6-week old females and males N:NIH(S)-*FoxI^{fl/fl}* mice that were provided from the Chair of Laboratory Animal, Veterinary School, National University of La Plata (Argentina).

Mice were inoculated subcutaneously (s. c.) into the right flank with 4×10^5 and 2×10^6 human osteosarcoma MG-63 cells. Tumor size was assessed using a caliper every 10 days after implantation and approximate tumor burden (mm^3) was calculated as $\text{length} \times \text{width}^2/2$ ($V = lw^2/2$), where length and width are the longest and shortest axes in millimeters.

For therapeutic experiments, mice were treated when the xenograft tumors reached 250 mm^3 . Mice ($n = 5$ animals per group) received an injection of 5 % DMSO in PBS (vehicle control mice), VOchrys (5.5 mg/kg, treated mice), and VOchrys (27.5 mg/kg, treated mice) via intraperitoneal every day for 11 days. Tumor growth was monitored by measuring tumor diameters every 3 days with a caliper, and animal weights were monitored at the same time.

Statistical analysis

Results are expressed as the mean of three independent experiments and plotted as mean \pm standard error of the

mean (SEM). The total number of repeats (n) is specified in the legends of the figures. Statistical differences were analyzed using the analysis of variance method followed by the test of least significant difference (Fisher).

The statistical analyses were performed using STAT-GRAPHICS Centurion XVII.I.

Results

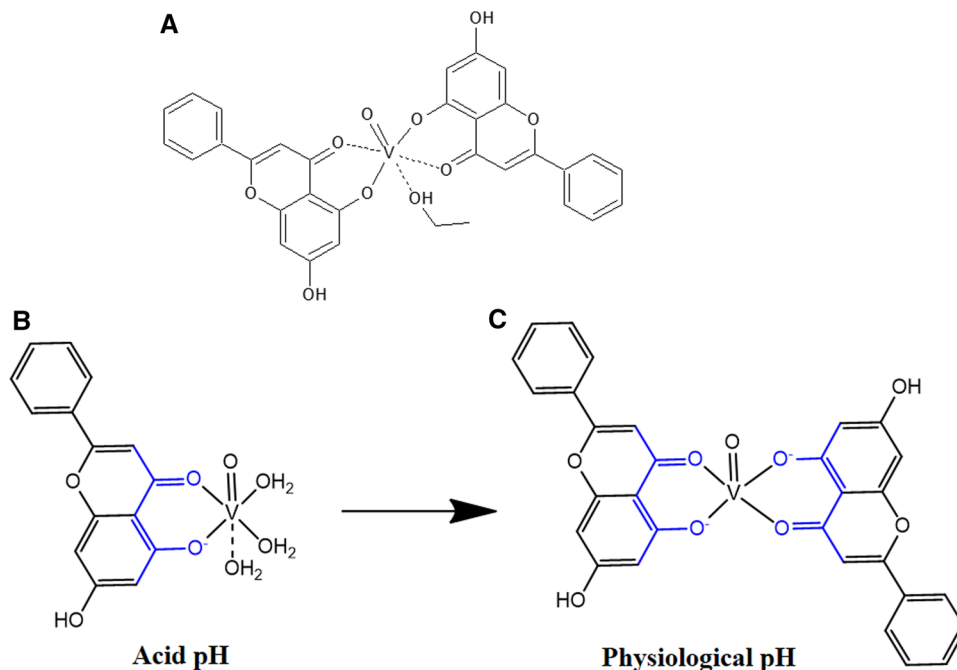
Synthesis and identification of VOchrys

VOchrys (Fig. 1) was synthesized according to Naso et al. [20]. The powder sample of the complex was identified by FTIR, and the main vibrations of the organic moiety as well as the coordinated vanadyl(IV) were compared with the previous report. Moreover, from the EPR data, it was assumed that in the proposed complex structure for VOchrys, one the axial positions is occupied by the oxygen atom of VO cation and the other by a solvent molecule. The equatorial positions are occupied by two organic ligand molecules.

Studying metal-based drugs is important to explore the properties of a potential “active species” and further uncovering the details associated with their specific composition and geometry likely important to the pharmacological action. Speciation is an important concept that assists researchers in understanding developments that involve metal ions [24].

In solution, it can be assumed that the main species of the complex is VOL_2 , taking into account the L/M ratio and the spectrophotometric titrations. Besides, the compound

Fig. 1 Vanadium complex structure. Chemical proposed structure of oxidovanadium(IV)-chrysin complex (a), monomeric configuration of oxidovanadium(IV)-chrysin complex under acid condition (b), and dimeric configuration of oxidovanadium(IV)-chrysin complex at physiological pH (c)



investigated herein has shown a very good stability at physiological pH, as it has been demonstrated by UV–Vis and EPR spectroscopy [20]. On the other hand, Sanna and col. have recently described that chrysin ligand form penta-coordinated structures (CO, O–) with “acetylaceton-like” coordination showing dimeric configuration of chrysin complex at physiological pH (see Fig. 1b, c) [25]. These acetylaceton-like structures show low interaction with different blood molecules keeping their structure, because they have good stability under physiological conditions [26].

3D in vitro studies

Development of MG-63 multicellular spheroids

Several scientific bibliographic reports show the potential uses of spheroids in cancer pharmacology [13, 27]. Three-dimensional cell culture contributes to either the elimination of non-effective drug candidates at the preclinical state or to the identification of promising drugs that would fail in classical monolayer (2D) assays. Therefore, we have developed a novel multicellular spheroids model using human osteosarcoma MG-63 cells by the hanging drop technique.

Figure 2a shows the growth of MG-63 spheroids after 5 days of culture.

The growth is lineal until the 2nd day with a volume value of $2 \times 10^6 \mu\text{m}^3$. From this day, it can be seen a more active proliferation correlated with the increase of volume value ($4.3 \times 10^6 \mu\text{m}^3$) until $5.6 \times 10^6 \mu\text{m}^3$ volume value in the 5th day.

Besides, after 5 days of growth, the spheroids reach a diameter of 400–420 μm . This size is the reported and recommended size for the assay to test drugs, since with this diameter, the spheroids express the main features of avascular solid tumors, such as hypoxia regions [28].

After 5 days of growth, the circularity values increase, because the edges of multicellular tumor spheroids (MCTS) are more regular and uniform, achieving a compact configuration similar to the cytoarchitecture of the solid osteosarcoma tumor (Fig. 2b).

Effects of VOchrys on the cell viability and morphology of MG-63 multicellular spheroids

To determine the antitumor effectiveness of VOchrys, we decided to evaluate its effects on cell viability in MG-63 multicellular spheroids using the acid phosphatase assay as a marker [22].

The acid phosphatase technique is a reliable tool used to determine the cell viability of multicellular spheroids in the antitumor drug screening [14].

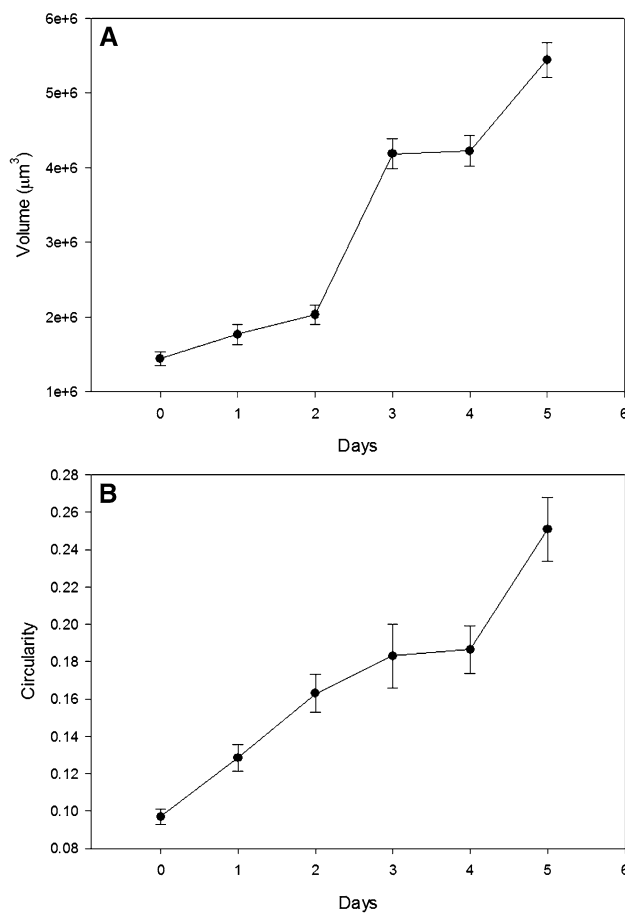


Fig. 2 **a** MG-63 multicellular spheroid growth curve expressed in μm^3 after 5 days of culture. The results are expressed as the volume (μm^3) and represent the mean \pm the standard error of the mean (SEM) ($n = 10$). **b** MG-63 multicellular spheroid circularity calculated using ImageJ 1.49B. The results are expressed as the circularity and represent the mean \pm the standard error of the mean (SEM) ($n = 10$)

Figure 3 shows the effects of VOchrys on cell viability in MG-63 multicellular spheroids. A loss of acid phosphatase, indicated by a decrease in the activity of this enzyme, was observed when MG-63 multicellular spheroids were exposed to 100 μM of VOchrys during 72 h. The data presented herein show a cytotoxic effect of VOchrys with statistically significant differences versus the control (basal condition) ($p < 0.01$).

On the other hand, as it can be seen in Fig. 4, the complex impaired the cell viability affecting the shape and volume of the spheroids. The values of shape corrected volume are approximately 1000 ± 56 and $261 \pm 17 \text{ mm}^3$ for the control and treatment, respectively ($p < 0.01$). These results are in agreement with the deleterious effect of VOchrys on MG-63 multicellular spheroids viability.

Fig. 3 Effects of VOchrys on the cell viability of MG-63 multicellular spheroids. Two spheroids were incubated in Dulbecco's modified Eagle's medium (DMEM) alone (basal) or with 100 μM of VOchrys at 37 $^{\circ}\text{C}$ for 72 h. Then, the acid phosphatase activity was measured as cell viability biomarker. The results are expressed as the percentage of the basal level and represent the mean \pm the standard error of the mean (SEM) ($n = 18$). Asterisk in comparison with the basal level ($p < 0.01$)

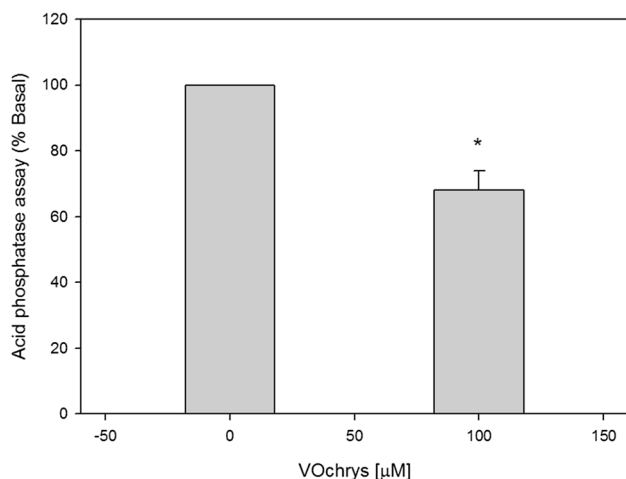
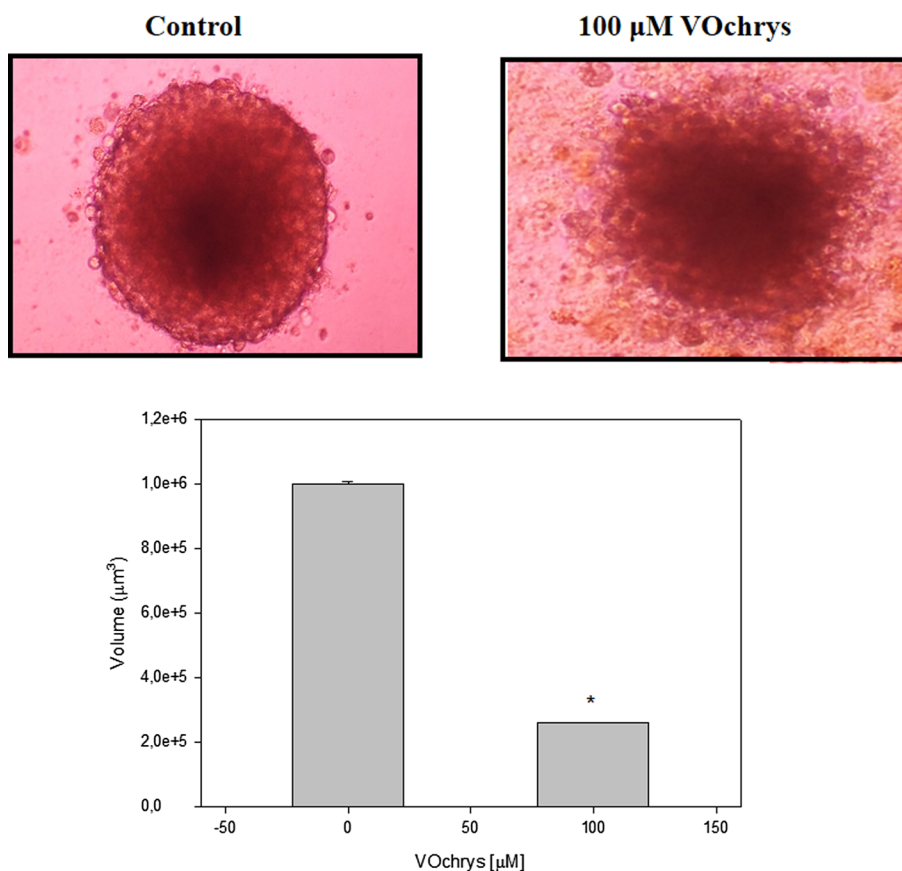


Fig. 4 Effects of VOchrys on the shape and volume of MG-63 multicellular spheroids. Representative images of control and treated spheroids are shown in the upper panel. The results are expressed as the percentage of the basal and represent the mean \pm the standard error of the mean (SEM) ($n = 10$). Asterisk significant difference in comparison with the basal conditions ($p < 0.01$)

In vivo studies

Development of a murine animal model N:NIH (S) FoxI^{nu} xenograft with MG-63 human osteosarcoma cells

The high quantity of worldwide investigation with several scientific reports registered in PubMed, and other medical databases emphasize the international interest for osteosarcoma research [29–31]. Partly, this is explained by the clinical inquiries that yet need to be answered on how to improve cancer patient care. On the other hand, it is the variable and complex genesis and physiology of osteosarcoma that attract scientists from diverse areas of expertise to study the biology and the pharmacology of this highly malignant bone neoplasm. Therefore, we create a new murine model to study alternative treatments for osteosarcoma. In this sense, with the main goal to evaluate the pharmacological properties of alternative antitumor agents, we proceeded to develop for the first time a new animal model with human osteosarcoma MG-63 cells.

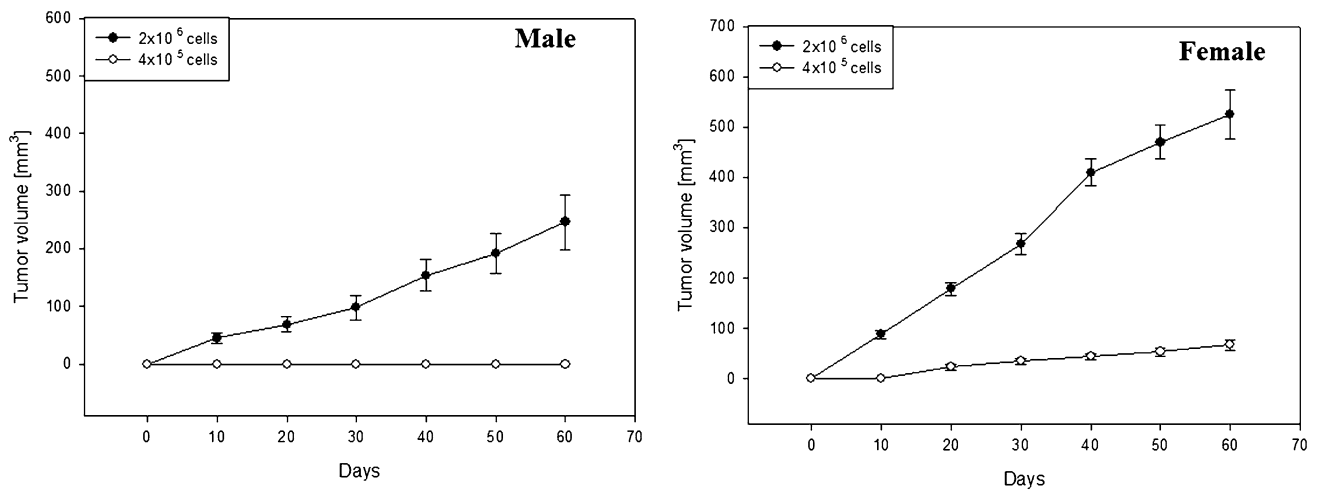


Fig. 5 Osteosarcoma tumor growth in athymic nude mice. Males and females (N:NIH (S) Fox1^{nu}) were inoculated subcutaneously with 4×10^5 and 2×10^6 cells per animal). Tumor size was assessed

using a caliper every day after implantation and approximate tumor volume (mm^3) were calculated as $\text{length} \times \text{width}^2/2$ ($V = lw^2/2$)

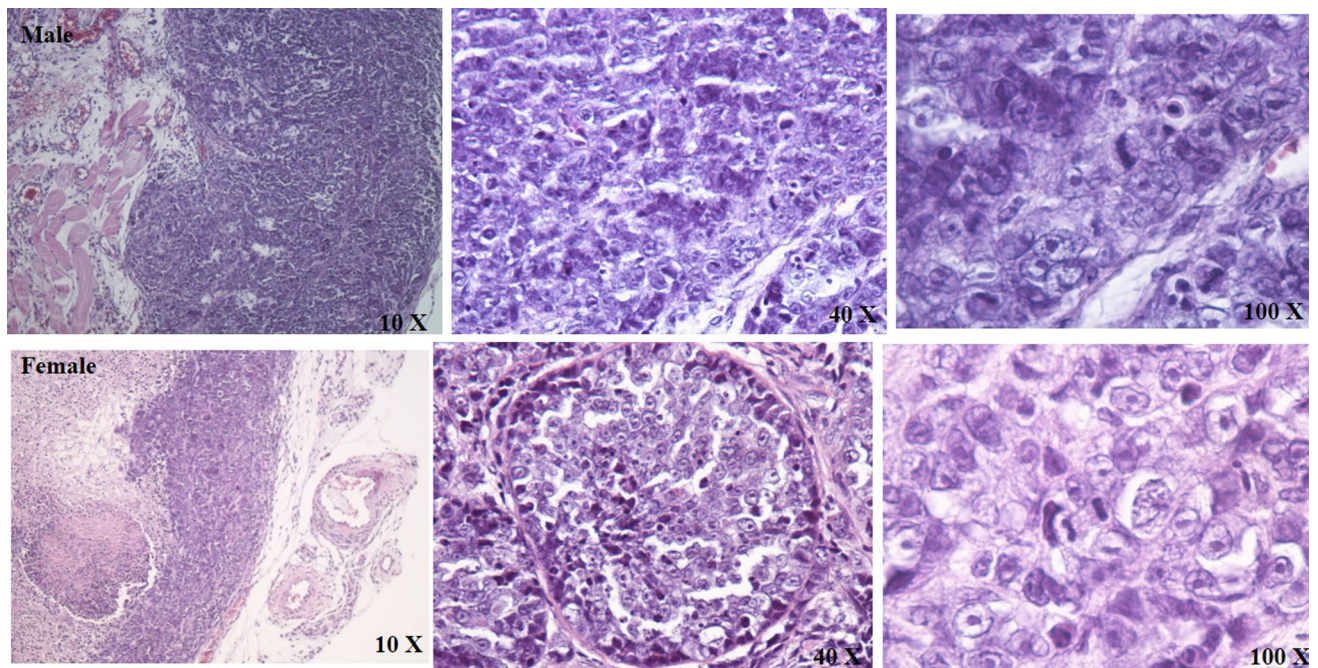


Fig. 6 Histopathology of tumor samples. *Upper panel* male tumor samples, *lower panel* female tumor samples. Tumor samples were dissected by scalpel and stained with hematoxylin/eosin. Magnifications $\times 10$, $\times 40$, and $\times 100$ are indicated

Females and males mice (N:NIH (S) Fox1^{nu}) were inoculated subcutaneously with different amounts of MG-63 cells (4×10^5 and 2×10^6 cells/animal) to normalize the best ratio of number of cells/tumor growth and its development.

Figure 5 shows the growth of osteosarcoma tumor in mice (N:NIH (S) Fox1^{nu}) as a function of time. As it can be seen, the male animals that were inoculated with 4×10^5

cells did not develop tumors, whilst the mice that were inoculated with 2×10^6 cells developed $246 \pm 47 \text{ mm}^3$ tumors after 60 days. On the other hand, the female animals developed tumors of 82 ± 14 and $562 \pm 39 \text{ mm}^3$ (animals inoculated with 4×10^5 and 2×10^6 cells, respectively) after 60 days.

Later, the tumor samples were collected and analyzed histopathologically with hematoxylin/eosin stain. It can be

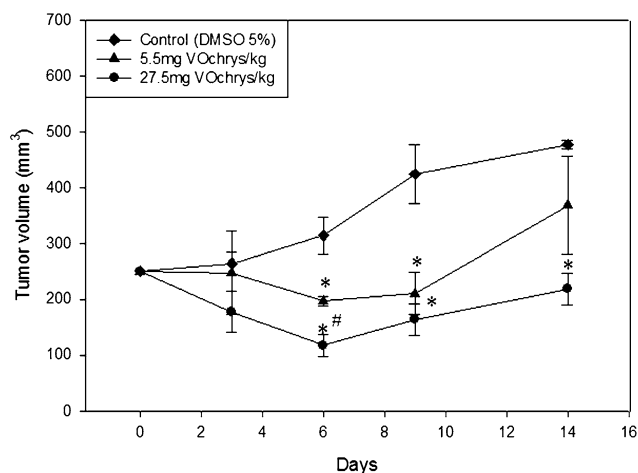


Fig. 7 In vivo antitumor effects of VOchrys. MG-63 cells were inoculated subcutaneously into the right flank of nude mice and allowed to form tumors, following which mice were assigned to each treatment groups [Control, VOchrys (5.5 mg/kg), and VOchrys (27.5 mg/kg)] as described in “Materials and methods”. Tumor volume was

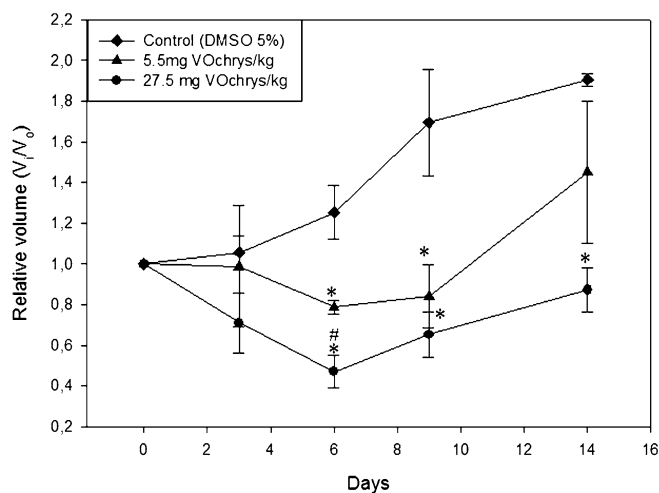
seen from Fig. 6 that it could be observed a focused deep tissue and neoplastic infiltration in the tumor samples from male animals (10×). Both 40× and 100× magnifications show in detail infiltrate of neoplastic cells with marked pleomorphism, macrokariosis, anisokaryosis, and evident nucleoli together with the aberrant presence of mitotic figures. In the case of females, infiltrated deep well defined and neoplastic tissue with necrosis areas can be observed at 10×, while at 40× and 100×, macrokariosis and anisokariosis were observed.

These results show that the osteosarcoma tumor in mice (N:NIH (S) Fox1tm) displays neoplastic morphological features related to these types of tumors.

VOchrys antitumor efficacy evaluation in athymic nude mice N:NIH(S) Fox1tm bearing human osteosarcoma tumor derived from MG-63 cell line

After to establish the tumor model line MG-63 in mice (N:NIH(S) Fox1tm), we decided to evaluate the in vivo antitumor effects of VOchrys, previously studied on in vitro systems. This compound had previously shown promising effects in a 2D culture system of osteosarcoma cells [32]. Therefore, it was interesting to evaluate its effects in vivo to analyze the possible clinical use of this vanadium based drug in an alternative therapy for osteosarcoma.

Due to the shorter time and best growth of tumor development in female mice, these animals were chosen to study the anticancer efficacy of this metallodrug. The treatment was performed during 11 consecutive days every 24 h and involved the following three groups of five animals



measured at the indicated time points after the onset of treatment. In relative volume, $V = \text{volume}$ and $V_0 = \text{initial volume}$. All data are presented as mean \pm SEM for five mice/group. * $p < 0.01$ with reference to basal, # $p < 0.01$ between treatments

Table 1 Effects of VOchrys on body weight in mice

	Animal body weight (Wc)
Control	24.33 \pm 0.88
5.5 mg VOchrys/kg	24.41 \pm 0.84
27.5 mg VOchrys/kg	24.25 \pm 0.75

Values are expressed as mean \pm SEM for five mice/group

each: DMSO 5 % in PBS (vehicle control mice), VOchrys (5.5 mg/kg, treated mice), and VOchrys (27.5 mg/kg, treated mice).

Figure 7 shows the in vivo antitumor effects of VOchrys in osteosarcoma mice model.

The result showed that from the 6th day of treatment, the tumor volume decreased with a difference statistically significant over the control for both treatments (* $p < 0.01$). After 6 days of treatment, it was observed that the treatment carried out with the highest dose of VOchrys produced a reduction of the tumor volume greater than the treatment with the lower concentration of vanadium complex, demonstrating the effect of concentration on the tumor volume reduction (# $p < 0.01$). In this sense, the values of tumor volume (mm³) were 314 \pm 32, 197 \pm 9, and 117 \pm 18 for control and treatments with 5.5 and 27.5 mg/kg, respectively. After 9 days of treatment, it was observed that both concentrations of VOchrys continue tumor reduction compared to the control conditions, obtaining values of tumor volume of 423 \pm 52, 210 \pm 38, and 165 \pm 28 mm³ for control and treatments, respectively (* $p < 0.01$). The last measurement of tumor size was performed on day 14th after 3 days of

the last dose of drug, for this time. As it can be seen, the tumor reduction could be determined only from treatment with the highest dose of vanadium drug.

On the other hand, VOchrys suppressed tumor growth in the nude mice without inducing toxicity and side effects (measured by the loss of body weight), as shown in Table 1. We did not observe any symptoms of toxicity (e.g., lethargy and decreased feeding).

These results demonstrate that the complex VOchrys caused a desired antitumor effect, since it reduced the tumor volume without affecting the animal health.

Discussion

Flavonoids are a large family of compounds synthesized by plants that have a common chemical structure [33]. These compounds are of great interest for their potential therapeutic effects on animals and human beings [34]. The modulation of flavonoid effects by complex formation to yield flavonoid–metal complexes is a very extensive field of interest. In fact, the pharmacological actions of these compounds are more effective than those of free flavonoids, meaning that the physiological and anticancer properties of flavonoids are enhanced on complexation with metal ions [32]. On the other hand, several vanadium compounds show interesting antitumor properties against several types of cancer, exhibiting higher anticancer activity than clinical reference drugs, such as cisplatin [8, 35, 36].

In vertebrates, higher amounts of vanadium are detected especially in bones than in other tissues [1]. We use the human osteosarcoma cell line MG-63 for the investigation of vanadium storage and bioactivity. This tumor cell line is a very good model to study the pharmacological actions, cytotoxicity, and genotoxicity as well as the putative mechanisms involved in the anticancer effects of new metal-based compounds [37].

One of the more widely used methodologies to culture 3D MCTS is the hanging drop technique. To achieve the growth of the MCTS, a drop of the cellular suspension is cultured in inverted substrates as culture plates [11, 38]. Besides the challenge of developing the model for each cell line, it is also necessary to set up the endpoint of the experiment and the way to determine it. Due to the complexity of the structure acquired by the MCTSs, it is difficult to apply the standard measurements of cell viability and it is fundamental to carry out a validation of the chosen or selected method. One of the most common systems to evaluate the viability of an MCTS widely employed in laboratories is the acid phosphatase method validated in a wide range of cell lines with high selectivity, reproducibility, and accuracy [14, 21]. The 3D tumor model of MG-63 osteosarcoma cell line can be mainly referred to Santini

et al. [39]. These authors use the method of liquid overlay for the spheroid formation, obtaining cellular aggregates, which are subjected to physical and chemical treatments to evaluate the damage on the spheroids. They have tested the effect of a magnetic field on spheroids demonstrating that there is no damage induced by this field or alterations in parameters, such as proteins, GSH/GSSG ratio, lactate dehydrogenase activity, and growth rate [40].

Our results in MG-63 human osteosarcoma cell line show a very good correlation between days of growth and multicellular spheroids formation, with similar features to those obtained for other cell lines [41–43].

Our previous results in MG-63 cell monolayers showed that VOchrys impaired the cell viability in a dose response manner from 10 to 100 μM , increasing the caspase-3 level and ROS generation. The compound decreased 35 and 80 % cell viability at 10 and 100 μM , respectively [32]. On the other hand, our findings in a 3D system show that VOchrys (100 μM) decreased the metabolic activity of spheroids diminishing 35 % of the acid phosphatase activity. Besides, the vanadium complex reduced the cell viability affecting the shape and volume of the spheroids. These results are very important, because the complex induced cytotoxicity using pharmacological appropriate concentration against human osteosarcoma cells in 2D and 3D models with very interesting effects. In this order, a scientific report has previously demonstrated that osteosarcoma cell spheres have resistance to cisplatin and doxorubicin treatments [44].

Schreiber-Brynzak and co-workers published the effects of different reference metal-based anticancer drugs, such as platinum, gallium, lanthanum, and ruthenium compounds against 2D and 3D colon and ovarian cancer models [28]. Detailed comparison of data obtained for all tested metal-based drugs shows that the use of 3D model results in a totally new ranking of compounds with regard to their cytotoxicity in vitro. The cytotoxicity of the gallium complex KP46 and the ruthenium derivate KP1339 was markedly lower in the 3D spheroid model than in monolayer showing IC_{50} values of 133 and 244 μM , respectively [28].

Besides, gemcitabine and 5-FU treatments only showed drug efficacy against pancreatic cancer spheroids at 200 μM [45].

The advantages of 3D spheroid-based experiments underline the necessity of using different experimental models for reliable preclinical investigations to assess and better predict the anticancer potential of new compounds [28].

In this way, animal models of different human cancers have evolved in attempts to represent the complexity of this disease. Human tumor xenograft models are the most widely used method to help the prediction of anticancer potency in preclinical studies [46].

These models have been employed to provide a better understanding of tumorigenesis progression, drug response, and drug resistance. Nevertheless, the available and highly specific experimental models possess some inherent limitations related to tumor stage, genetic background, and growth conditions [47].

Therefore, the development of new xenograft osteosarcoma models is a very interesting field of research in cancer drug discovery. For the first time, we have developed a new human osteosarcoma xenograft mice model using MG-63 cells. Our results show that the female animals developed higher tumors in a shorter time than male mice, whereby we use the female animals to evaluate the antitumor efficacy of VOchrys against osteosarcoma.

The *in vivo* anticancer effects of VOchrys showed that this compound reduced the tumor volume in xenograft mice. After 6 days of treatment, the values of tumor volume were 314 ± 32 , 197 ± 9 , and 117 ± 18 mm³ for control and treatments with 5.5 and 27.5 mg/kg, respectively. After 9 days of treatment, it was observed that both treatments with VOchrys suppress the tumor growth obtaining values of tumor volume of 423 ± 52 , 210 ± 38 and 165 ± 28 mm³ for control and treatments, respectively. Besides, other very important pharmacological point is that VOchrys reduced tumor growth in the nude mice without inducing toxicity and side effects (e.g., lethargy, decreased feeding, etc).

These results demonstrate that the complex VOchrys shows promissory anticancer actions, since it reduced the tumor volume without affecting the animal health.

Different animal studies have shown that vanadium is effective in preventing and reducing neoplastic developments in several types of cancer (see Table S1) [48–53].

Moreover, several scientific reports have also described the putative therapeutic effects of vanadium on the growth and metastatic potential of tumor cells in xenograft mice models [6, 54].

The *in vivo* effects of VOchrys on the osteosarcoma xenograft mice model are reported herein for the first time, and it is relevant for the *in vivo* effects of vanadium compounds on xenograft osteosarcoma model.

Conclusion

Determination of the main features of the tumor models used in pharmacological studies is very important to understand the interactions between drugs and cellular architecture and components of cancer.

Characterisation of tumor models can be carried out using different techniques. Currently, research in this area shows a tendency from relatively simple monolayer or 2D systems used for preclinical screening towards the 3D model systems which are more suitable for understanding the complex

environment of solid tumors. Solid tumors are characterised by heterogeneous cell populations and complex three-dimensional architecture. This complex structure implies gradients of nutrients, metabolites, and drugs between the tumor and its microenvironment. These factors strongly influence cellular uptake and drug intra-tumour distribution.

The present work deals with the development of a 3D multicellular spheroid model of osteosarcoma and of an *in vivo* murine model of xenograft mice bearing a human osteosarcoma cell line MG-63, both specially appropriate to test different compounds with perspectives as anticancer agents. In the present manuscript, an MCTS model of MG-63 human osteosarcoma cell line was used to characterize the ability of a vanadium(IV) complex with the flavonoid chrysin, VOchrys to reduce the viability of the MCTS model. This vanadium complex had been previously tested in a 2D monolayer system of the same tumor cell line, showing anticancer activity even higher than cis-Pt. In the 3D MCTS system, VOchrys also displayed antitumor actions, since it altered the shape of spheroids and decreased the viability of them. Moreover, when the complex was tested in the *in vivo* xenograft mice model, important antitumor actions were observed along the treatment. The pharmacological effects were determined through a significant reduction of the tumor volume and suppression of the tumor growth along 11 days of treatment without any symptom affecting the health and behaviour of the animals.

The results obtained and discussed in detail in the present work demonstrated the advantages of the MCTS system and the *in vivo* xenograft mice model to evaluate the anticancer efficacy of VOchrys, allowing to place it in the threshold of non-platinum antitumor drugs.

Acknowledgments This work was partly supported by UNLP (11X/690), CONICET (PIP 1125), and ANPCyT (PICT 2014-2223, PPL2-2011-0008, and PME 2006-068) from Argentina. IEL and SBE are members of the Carrera del Investigador, CONICET, Argentina. JFCV is fellowship from CONICET, Argentina. The authors would like to thank to Prof. Dr. Adriana Massone (FCV, UNLP) for the management work with the tumor histopathology.

References

1. Nielsen FH (1995) Metal ions in biological systems: volume 31: vanadium and its role for life. CRC Press, Boca Raton
2. Willsky GR, Chi LH, Godzala M et al (2011) Anti-diabetic effects of a series of vanadium diphosphate complexes in rats with streptozotocin-induced diabetes. *Coord Chem Rev* 255:2258–2269. doi:10.1016/j.ccr.2011.06.015
3. Thompson KH, Orvig C (2006) Metal complexes in medicinal chemistry: new vistas and challenges in drug design. *Dalton Trans.* doi:10.1039/b513476e
4. Thompson KH, Lichter J, LeBel C et al (2009) Vanadium treatment of type 2 diabetes: a view to the future. *J Inorg Biochem* 103:554–558. doi:10.1016/j.jinorgbio.2008.12.003

5. Etcheverry SB, Barrio DA (2007) Vanadium and bone: relevance of vanadium compounds in bone cells. In: Kustin K, Costa Pesoa J, Crans DC (eds) Vanadium: the versatile metal, chap 15, vol 974. American chemical society series, pp 204–216
6. Evangelou AM (2002) Vanadium in cancer treatment. *Crit Rev Oncol Hematol* 42:249–265
7. Kioseoglou E, Petanidis S, Gabriel C, Salifoglou A (2015) The chemistry and biology of vanadium compounds in cancer therapeutics. *Coord Chem Rev*. doi:10.1016/j.ccr.2015.03.010
8. Rehder D (2012) The potentiality of vanadium in medicinal applications. *Future Med Chem* 4:1823–1837. doi:10.4155/fmc.12.103
9. Pessoa JC, Etcheverry S, Gambino D (2014) Vanadium compounds in medicine. *Coord Chem Rev*. doi:10.1016/j.ccr.2014.12.002
10. Gorlick R, Khanna C (2010) Osteosarcoma. *J Bone Miner Res* 25:683–691. doi:10.1002/jbmr.77
11. Page H, Flood P, Reynaud EG (2013) Three-dimensional tissue cultures: current trends and beyond. *Cell Tissue Res* 352:123–131. doi:10.1007/s00441-012-1441-5
12. Ho WY, Yeap SK, Ho CL et al (2012) Development of multicellular tumor spheroid (MCTS) culture from breast cancer cell and a high throughput screening method using the MTT assay. *PLoS One* 7:e44640. doi:10.1371/journal.pone.0044640
13. Benien P, Swami A (2014) 3D tumor models: history, advances and future perspectives. *Future Oncol* 10:1311–1327. doi:10.2217/fon.13.274
14. Friedrich J, Eder W, Castaneda J et al (2007) A reliable tool to determine cell viability in complex 3-d culture: the acid phosphatase assay. *J Biomol Screen* 12:925–937. doi:10.1177/1087057107306839
15. Modok S, Scott R, Alderden RA et al (2007) Transport kinetics of four- and six-coordinate platinum compounds in the multi-cell layer tumour model. *Br J Cancer* 97:194–200. doi:10.1038/sj.bjc.6603854
16. Alderden RA, Mellor HR, Modok S et al (2007) Elemental tomography of cancer-cell spheroids reveals incomplete uptake of both platinum(II) and platinum(IV) complexes. *J Am Chem Soc* 129:13400–13401. doi:10.1021/ja076281t
17. Zhang JZ, Bryce NS, Siegle R et al (2012) The use of spectroscopic imaging and mapping techniques in the characterisation and study of DLD-1 cell spheroid tumour models. *Integr Biol (Camb)* 4:1072–1080. doi:10.1039/c2ib20121f
18. Céspedes MV, Casanova I, Parreño M, Mangués R (2006) Mouse models in oncogenesis and cancer therapy. *Clin Transl Oncol* 8:318–329
19. Francia G, Cruz-Munoz W, Man S et al (2011) Mouse models of advanced spontaneous metastasis for experimental therapeutics. *Nat Rev Cancer* 11:135–141. doi:10.1038/nrc3001
20. Naso L, Ferrer EG, Lezama L et al (2010) Role of oxidative stress in the antitumor action of a new vanadyl(IV) complex with the flavonoid chrysin in two osteoblast cell lines: relationship with the radical scavenger activity. *J Biol Inorg Chem* 15:889–902. doi:10.1007/s00775-010-0652-z
21. Friedrich J, Seidel C, Ebner R, Kunz-Schughart LA (2009) Spheroid-based drug screen: considerations and practical approach. *Nat Protoc* 4:309–324. doi:10.1038/nprot.2008.226
22. Hirschhaeuser F, Menne H, Dittfeld C et al (2010) Multicellular tumor spheroids: an underestimated tool is catching up again. *J Biotechnol* 148:3–15. doi:10.1016/j.jbiotec.2010.01.012
23. National Research Council (2011) Guide for the Care and Use of Laboratory Animals. National Academies Press, Washington, D.C.
24. Crans DC, Woll KA, Prusinskas K et al (2013) Metal speciation in health and medicine represented by iron and vanadium. *Inorg Chem* 52:12262–12275. doi:10.1021/ic4007873
25. Sanna D, Ugone V, Lubinu G et al (2014) Behavior of the potential antitumor VIVO complexes formed by flavonoid ligands. 1. Coordination modes and geometry in solution and at the physiological pH. *J Inorg Biochem* 140:173–184. doi:10.1016/j.jinorgbio.2014.07.007
26. Sanna D, Micera G, Garribba E (2010) New developments in the comprehension of the biotransformation and transport of insulin-enhancing vanadium compounds in the blood serum. *Inorg Chem* 49:174–187. doi:10.1021/ic9017213
27. Thoma CR, Zimmermann M, Agarkova I et al (2014) 3D cell culture systems modeling tumor growth determinants in cancer target discovery. *Adv Drug Deliv Rev* 69–70:29–41. doi:10.1016/j.addr.2014.03.001
28. Schreiber-Brynzak E, Klapproth E, Unger C et al (2015) Three-dimensional and co-culture models for preclinical evaluation of metal-based anticancer drugs. *Invest New Drugs* 33:835–847. doi:10.1007/s10637-015-0260-4
29. Ren L, Mendoza A, Zhu J et al (2015) Characterization of the metastatic phenotype of a panel of established osteosarcoma cells. *Oncotarget* 6:29469–29481
30. Luetke A, Meyers PA, Lewis I, Juergens H (2014) Osteosarcoma treatment—where do we stand? A state of the art review. *Cancer Treat Rev* 40:523–532. doi:10.1016/j.ctrv.2013.11.006
31. Isakoff MS, Bielack SS, Meltzer P, Gorlick R (2015) Osteosarcoma: current treatment and a collaborative pathway to success. *J Clin Oncol*. doi:10.1200/JCO.2014.59.4895
32. Leon IE, Di Virgilio AL, Porro V et al (2013) Antitumor properties of a vanadyl(IV) complex with the flavonoid chrysin [VO(chrysin)₂EtOH]₂ in a human osteosarcoma model: the role of oxidative stress and apoptosis. *Dalton Trans* 42:11868–11880. doi:10.1039/c3dt50524c
33. Beecher GR (2003) Overview of dietary flavonoids: nomenclature, occurrence and intake. *J Nutr* 133:3248S–3254S
34. Jafari S, Saeidnia S, Abdollahi M (2014) Role of natural phenolic compounds in cancer chemoprevention via regulation of the cell cycle. *Curr Pharm Biotechnol* 15:409–421
35. Reytman L, Braitbard O, Hochman J, Tshuva EY (2015) Highly effective and hydrolytically stable vanadium(V) amino phenolato antitumor agents, pp 1–9. doi:10.1021/acs.inorgchem.5b02519
36. León IE, Cadavid-Vargas JF, Tiscornia I et al (2015) Oxidovanadium(IV) complexes with chrysin and silibinin: anticancer activity and mechanisms of action in a human colon adenocarcinoma model. *J Biol Inorg Chem* 20:1175–1191. doi:10.1007/s00775-015-1298-7
37. Mohseny AB, Hogendoorn PCW, Cleton-Jansen A-M (2012) Osteosarcoma models: from cell lines to zebrafish. *Sarcoma* 2012:417271. doi:10.1155/2012/417271
38. Kelm JM, Timmins NE, Brown CJ et al (2003) Method for generation of homogeneous multicellular tumor spheroids applicable to a wide variety of cell types. *Biotechnol Bioeng* 83:173–180. doi:10.1002/bit.10655
39. Santini M, Rainaldi G, Indovina P (2000) Apoptosis, cell adhesion and the extracellular matrix in the three-dimensional growth of multicellular tumor spheroids. *Crit Rev Oncol* 36:75–87
40. Santini MT, Rainaldi G, Ferrante A et al (2006) A 50 Hz sinusoidal magnetic field does not damage MG-63 three-dimensional tumor spheroids but induces changes in their invasive properties. *Bioelectromagnetics* 27:132–141. doi:10.1002/bem.20184
41. Bjørge L, Junnikkala S, Kristoffersen EK et al (1997) Resistance of ovarian teratocarcinoma cell spheroids to complement-mediated lysis. *Br J Cancer* 75:1247–1255
42. Vinci M, Gowan S, Boxall F et al (2012) Advances in establishment and analysis of three-dimensional tumor spheroid-based functional assays for target validation and drug evaluation. *BMC Biol* 10:29. doi:10.1186/1741-7007-10-29

43. Liu W-D, Zhang T, Wang C-L et al (2012) Sphere-forming tumor cells possess stem-like properties in human fibrosarcoma primary tumors and cell lines. *Oncol Lett* 4:1315–1320. doi:[10.3892/ol.2012.940](https://doi.org/10.3892/ol.2012.940)
44. Fujii H, Honoki K, Tsujiuchi T et al (2009) Sphere-forming stem-like cell populations with drug resistance in human sarcoma cell lines. *Int J Oncol* 34:1381–1386
45. Wen Z, Liao Q, Hu Y et al (2013) A spheroid-based 3-D culture model for pancreatic cancer drug testing, using the acid phosphatase assay. *Braz J Med Biol Res* 46:634–642. doi:[10.1590/1414-431X20132647](https://doi.org/10.1590/1414-431X20132647)
46. Langdon SP (2012) Animal modeling of cancer pathology and studying tumor response to therapy. *Curr Drug Targets* 13:1535–1547
47. Ek ETH, Dass CR, Choong PFM (2006) Commonly used mouse models of osteosarcoma. *Crit Rev Oncol Hematol* 60:1–8. doi:[10.1016/j.critrevonc.2006.03.006](https://doi.org/10.1016/j.critrevonc.2006.03.006)
48. El-Naggar MM, El-Waseef AM, El-Halafawy KM, El-Sayed IH (1998) Antitumor activities of vanadium(IV), manganese(IV), iron(III), cobalt(II) and copper(II) complexes of 2-methylamino-pyridine. *Cancer Lett* 133:71–76
49. Köpf-Maier P (1982) Development of necroses, virus activation and giant cell formation after treatment of Ehrlich ascites tumor with metallocene dichlorides. *J Cancer Res Clin Oncol* 103:145–164
50. Samanta S, Swamy V, Suresh D et al (2008) Protective effects of vanadium against DMH-induced genotoxicity and carcinogenesis in rat colon: removal of O(6)-methylguanine DNA adducts, p53 expression, inducible nitric oxide synthase downregulation and apoptotic induction. *Mutat Res* 650:123–131. doi:[10.1016/j.mrgentox.2007.11.001](https://doi.org/10.1016/j.mrgentox.2007.11.001)
51. Chakraborty T, Ghosh S, Datta S et al (2003) Vanadium suppresses sister-chromatid exchange and DNA-protein crosslink formation and restores antioxidant status and hepatocellular architecture during 2-acetylaminofluorene-induced experimental rat hepatocarcinogenesis. *J Exp Ther Oncol* 3:346–62
52. Bishayee A, Chatterjee M (1994) Inhibition of altered liver cell foci and persistent nodule growth by vanadium during diethylnitrosamine-induced hepatocarcinogenesis in rats. *Anticancer Res* 15:455–61
53. Wu Y, Ma Y, Xu Z et al (2014) Sodium orthovanadate inhibits growth of human hepatocellular carcinoma cells in vitro and in an orthotopic model in vivo. *Cancer Lett* 351:108–116. doi:[10.1016/j.canlet.2014.05.018](https://doi.org/10.1016/j.canlet.2014.05.018)
54. Bishayee A, Waghay A, Patel MA, Chatterjee M (2010) Vanadium in the detection, prevention and treatment of cancer: the in vivo evidence. *Cancer Lett* 294:1–12. doi:[10.1016/j.canlet.2010.01.030](https://doi.org/10.1016/j.canlet.2010.01.030)